Revista Mexicana de Física
ISSN: 0035-001X
rmf@ciencias.unam.mx
Sociedad Mexicana de Física A.C.
México

Chokprasombat, K.; Sirisathitkul, C.; Harding, P.; Chandarak, S.; Yimnirun, R.
Monodisperse magnetic nanoparticles: Effects of surfactants on the reaction between iron acetylacetonate and platinum acetylacetonate
Revista Mexicana de Física, vol. 59, núm. 3, mayo-junio, 2013, pp. 224-228
Sociedad Mexicana de Física A.C.
Distrito Federal, México

Monodisperse magnetic nanoparticles: Effects of surfactants on the reaction between iron acetylacetonate and platinum acetylacetonate

K. Chokprasombat[a], C. Sirisathitkul[a,*], P. Harding[a], S. Chandarak[b], and R. Yimnirun[b]
[a]*Molecular Research Unit, School of Science, Walailak University, Nakhon Si Thammarat 80161,Thailand.*
[b]*School of Physics, Institute of Science, Suranaree University of Technology and Synchrotron Light Research Institute (Public Organization), Nakhon Ratchasima 30000, Thailand,*
Tel: +66-75-672-945
**e-mail: schitnar@wu.ac.th;*

Received 16 October 2012; accepted 6 February 2013

Magnetic properties of monodisperse nanoparticles for ultrahigh density recording and biomedical applications are sensitive to their shape and size distributions. These attributes are, in turns, dictated by several parameters during the synthesis and heat treatments. In this work, monodisperse FePt-based magnetic nanoparticles around 5 nm in diameter were synthesized by the reaction between iron acetylacetonate ($Fe(acac)_3$) and platinum acetylacetonate ($Pt(acac)_2$) in benzyl ether. X-ray absorption near-edge structure (XANES) spectra agreed with transmission electron microscopy (TEM) and energy dispersive X-ray spectroscopy (EDS) that as-synthesized nanoparticles were composed of Pt-rich nuclei and iron oxides. Whereas their composition and size was not sensitive to the variation in the amount of surfactants (oleic acid and oleylamine), the nanoparticles exhibited a larger variation in shape with the increase in each surfactant from 1.5 to 4.5 mmol. After annealing in argon atmosphere at 650°C for 1 hour, the nanoparticles tended to agglomerate. Higher amounts of surfactants surrounded the nanoparticles apparently allowed more sintering because the decomposed carbon from the excess surfactants facilitated the reduction of iron oxides. More Fe in the large annealed particles then resulted in ferromagnetic properties. By contrast, the ferromagnetic behavior and the highest coercivity were obtained without such agglomeration in the case of annealed particles synthesized by using the minimum surfactants.

Keywords: Magnetic nanoparticles; Modified polyol process; Oleic acid; Oleylamine.

PACS: 75.75.-c; 75.50.Bb

1. Introduction

Many potential applications of monodisperse magnetic nanoparticles including biomedical diagnostics and therapy, high performance permanent magnets and ultrahigh density magnetic recording media have been suggested [1,2]. FePt nanoparticles with face-centered tetragonal (fct) phase are currently under investigations owing to their good chemical stability and high magnetocrystalline anisotropy [3]. Self-assembly of these ferromagnetic FePt nanoparticles is a promising candidate for manufacturing the magnetic bit patterned media for future hard disk drives. However, a synthetic procedure to obtain desirable morphology, proper composition and preferred easy axis is still not conclusive. Furthermore, the need of high temperature annealing to transform particles to the fct phase usually leads to particle agglomeration.

The synthesis of FePt nanoparticles commonly involves the thermal decomposition of iron pentacarbonyl ($Fe(CO)_5$) and the reduction of platinum(II) acetylacetonate ($Pt(acac)_2$) by polyalcohol in ether solvent. The particles are stabilized by surfactants (*e.g.* oleic acid and oleylamine) [3]. Many synthetic conditions such as the concentration of surfactants, heating rate, and type of solvent must be carefully adjusted to achieve high quality nanoparticles. It is well known that $Fe(CO)_5$ is very toxic, volatile and highly flammable. Moreover, the composition control of the particles is difficult due to the high volatility of the $Fe(CO)_5$, which remains in the vapour mixture during the synthesis. Yu et al. showed that the synthesis by using $Fe(CO)_5$ led to particle composition variation from 21 to 70 at.% Fe [4].

Alternatively, the co-reduction of less toxic iron(III) acetylacetonate ($Fe(acac)_3$) or iron(II) acetylacetonate ($Fe(acac)_2$) with $Pt(acac)_2$ has been employed [5-13]. The particles synthesized from this modified polyol process are generally smaller than those obtained by using $Fe(CO)_5$. Particles as small as 2 nm in diameter can be produced [10]. Furthermore, Nakaya et al. successfully synthesized the nanoparticles of about 5-6 nm in diameter by using excess surfactants in an absence of conventional ether solvents [8]. Although the FePt nanoparticles with a narrow size distribution have been synthesized by using $Fe(acac)_3$, the morphology and composition of the particles have not been effectively controlled. According to the heterocoagulation mechanism recently proposed by Beck Jr. *et al.* [12], the FePt nanoparticles are formed by the reduction of iron species on the surface of Pt nuclei. This involved the CO-spillover process and the Fe atoms at the surface were diffused into the particle by heating at high temperature. Taken this model into account, we have synthesized monodisperse nanoparticles by using an excess amount of $Fe(acac)_3$ and surfactants. The effect of the surfactants on the morphology of the nanoparticles before and after heat treatments can then be studied.

2. Experimental

In a modified polyol process using standard Schlenk line technique in N_2 atmosphere, 1.0 mmol $Fe(acac)_3$ and 0.5 mmol $Pt(acac)_2$ were mixed in 20 mL benzyl ether with the presence of oleic acid and oleylamine. Four samples designated as S1, S2, S3, and S4 were prepared by varying the amount of oleic acid and oleylamine as 1.5, 2.5, 3.5 and 4.5 mmol respectively. Each mixture was heated to reflux at 300°C for 3 hours before cooled down to room temperature under N_2 blanket. Ethanol (40 mL) was added to the reaction flask then the black product was centrifuged (5000 rpm, 15 min) to separate the particles. The brown supernatant was discarded and the precipitates were dispersed in 30 mL hexane. Small amount of ethanol ($\sim$ 5 mL) was added to the dispersion and the dispersion was centrifuged to remove large precipitates. Large precipitates were discarded and the black dispersion was mixed with more ethanol ($\sim$ 40 mL) and then centrifuged to precipitate the particles. To purify the particles, the precipitate was redispersed in hexane, precipitated with extra ethanol, and isolated by centrifuging twice. The final precipitates were dispersed in hexane ($\sim$30 mL) with the presence of small amount of oleic acid ($\sim$0.05 mL) and oleylamine ($\sim$0.05 mL), followed by purging with N_2 to remove O_2. The dispersion was stored in glass bottles in a refrigerator at 4°C. Morphology of the samples was examined by transmission electron microscopy (TEM) at an accelerating voltage of 200 kV and the particle composition was determined by energy dispersive X-ray spectroscopy (EDS). Magnetic properties were measured by vibrating sample magnetometry (VSM). Before the measurement, the colloids were dropped on silicon substrates and the

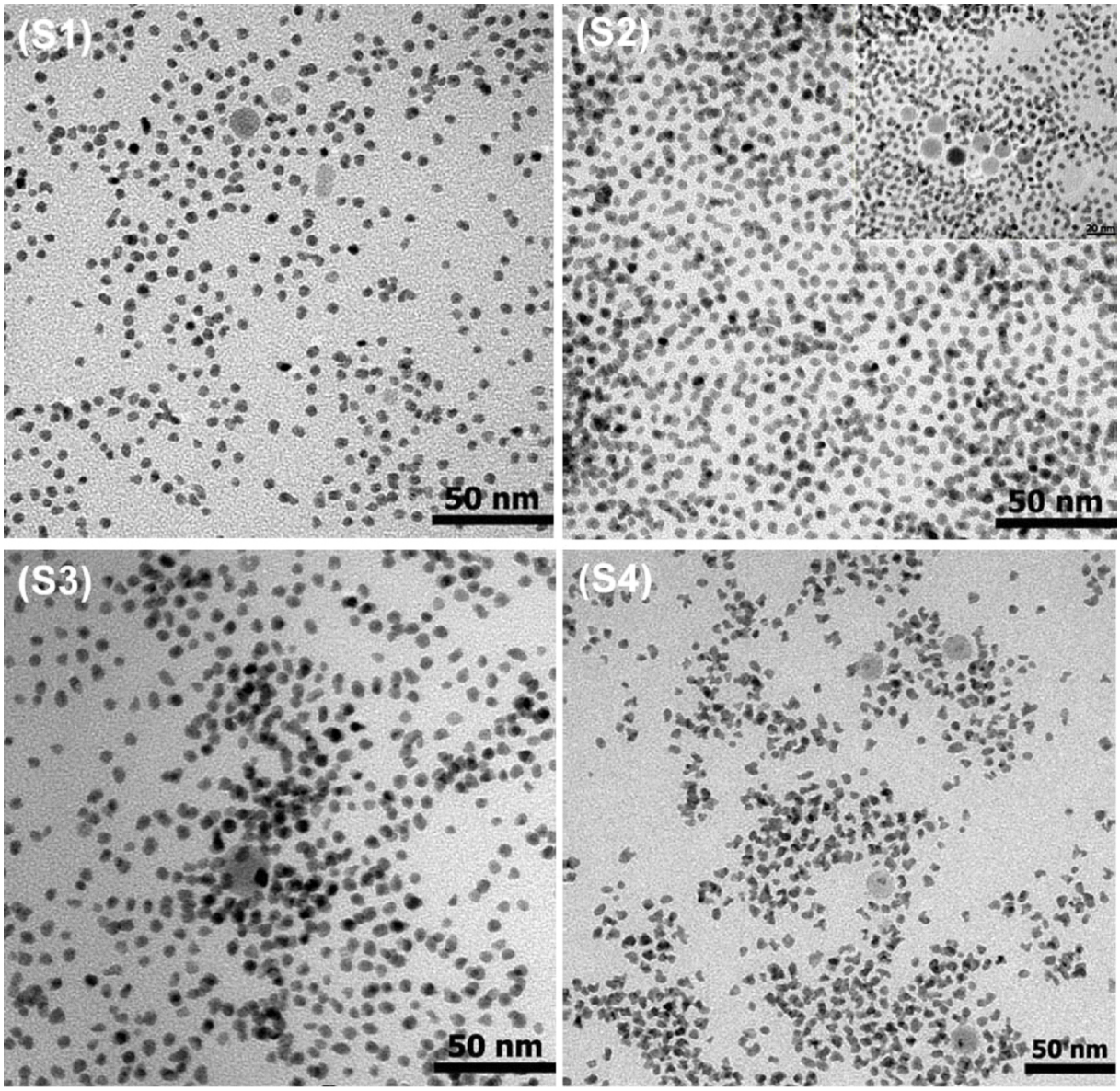

FIGURE 1. TEM images of as-synthesized nanoparticles using (S1) 1.5, (S2) 2.5, (S3) 3.5, and (S4) 4.5 mmol of each surfactant.

solvent was allowed to evaporate at room temperature. In order to examine the magnetic properties after annealing, a separated batch of dried colloid on silicon substrates was annealed in a tube furnace in Ar atmosphere at 650°C for 1 hour with a heating rate ≈ 10°C/min. The phase after this annealing was characterized by X-ray diffractometry (XRD). X-ray absorption spectroscopy (XAS) was obtained using synchrotron radiation at BL-8, Synchrotron Light Research Institute, Thailand. The X-ray absorption near-edge structure (XANES) measurements of Fe K-edge and Pt M_5-edge were performed in the fluorescence mode with the electron energy of 1.2 GeV and the electron current between 80 mA and 140 mA.

3. Results and discussion

TEM images of as-synthesized nanoparticles using $Fe(acac)_3$:$Pt(acac)_2$ ratio of 2:1 with varying amounts of each surfactant as 1.5, 2.5, 3.5 and 4.5 mmol are shown in Fig. 1. The nanoparticles of varying shapes around 5 nm in size are obtained in all samples. In a previous report by Nandwana *et al*. [10], the particle size obtained from using $Fe(CO)_5$ as a starting material was increased with increasing surfactant concentrations. By contrast, the size of particle around 2 nm did not vary with the surfactant concentration and heating rate when $Fe(CO)_5$ was replaced by $Fe(acac)_3$. In that case, such small particles were likely originated from quick nucleations and precursor depletions at the early state of the reaction. With a domination of the nucleation rate over the growth rate, the particles of size around 2 nm were then obtained [10]. The particles synthesized in our experiments are larger, probably due to the presence of excess surfactants at the room temperature (in [10], the surfactants were added at 120°C). The nucleation rate is decreased leading to the larger particles. Whereas the particle size is not sensitive to the change in surfactants from 1.5 to 4.5 mmol, the particles tend to exhibit a larger variation in shape when the amount of surfactants is increased. Interestingly, a few spheroid nanoparticles around 10 nm in diameter are also observed in the TEM images as exemplified by the inset of S2 in Fig. 1. Because of the double amount of $Fe(acac)_3$ used, these larger particles are likely iron oxides which are formed in the early state of the particle formation but could not be reduced and incorporated into the Pt nuclei.

The compositions of samples S1-S4 measured by EDS are compared in Table I. The atomic percentage of Fe is much lower than that of Pt. Furthermore, slightly above 20% O is also found in all samples. These evidences support the notion that the as-synthesized particles are mainly composed of Pt-rich nanoparticles and iron oxides either as a separated phase or a shell around a Pt-rich core. A large fraction Fe are apparently removed by the centrifugation of large iron oxide precipitates which explains a much lower Fe:Pt ratio than their initial molar ratio. The particle composition did not have a large variation with the change in surfactant concentration. By contrast, Sebt *et al*. founded that the increase in an amount of oleylamine reduced the Pt fraction obtained from the reaction between iron(II) chloride tetrahydrate ($FeCl_2{\cdot}4H_2O$) and $Pt(acac)_2$ with superhydride and 1,2 hexadecanediol as reducing agents [14]. The heterocoagulation mechanism suggests that the reduction process occurs on the surface of Pt-rich nanoparticles. The surface area of the nanoparticles which is dependent on the surfactant concentration should then regulate an efficiency of the reduction process. However, because samples S1-S4 are not substan-

TABLE I. Composition of as-synthesized nanoparticles measured by EDS.

Sample	Amount of the surfactants (mmol)		Atomic Percentage Percentage		
	Oleic acid	Oleylamine	Fe	Pt	O
S1	1.5	1.5	15.35	61.57	23.08
S2	2.5	2.5	20.11	58.19	21.70
S3	3.5	3.5	15.47	61.23	23.31
S4	4.5	4.5	18.53	57.61	23.86

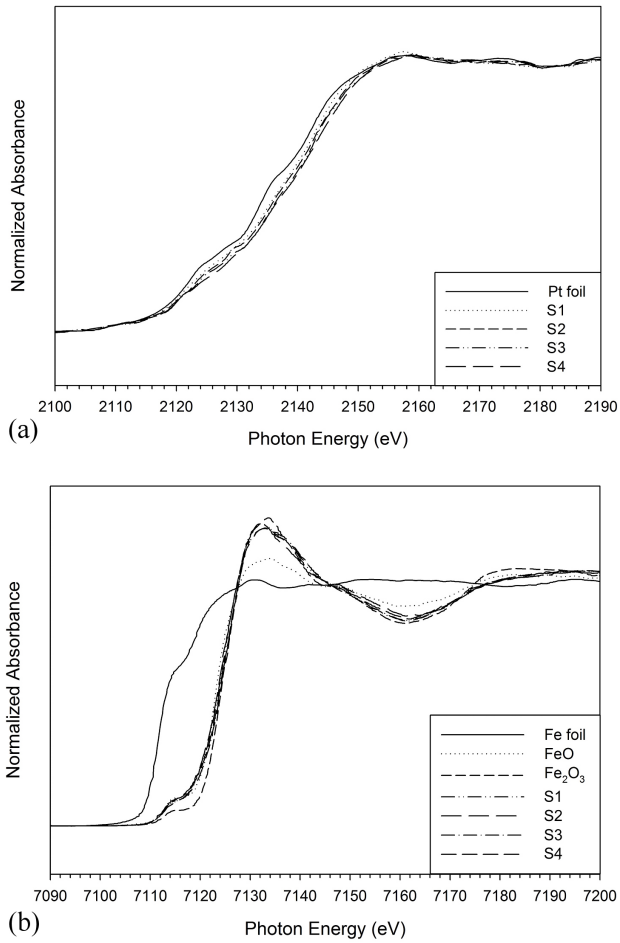

FIGURE 2. XANES spectra of as-synthesized nanoparticles (samples S1-S4); (a) Pt M_5-edge and (b) Fe K-edge.

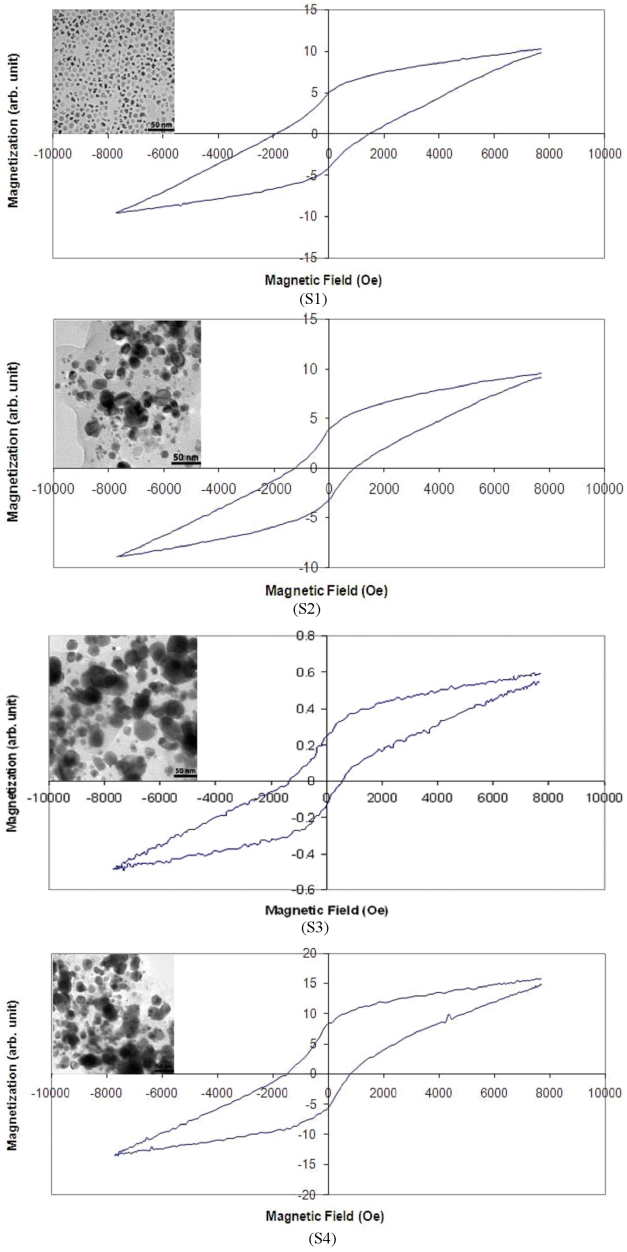

FIGURE 3. Magnetic hysteresis loops and TEM images (insets) of nanoparticles synthesized by using (S1) 1.5, (S2) 2.5, (S3) 3.5, and (S4) 4.5 mmol of each surfactant after the annealing at 650°C for 1 hour.

tially different in size, the effect of surfactant concentration on the composition is not marked.

The Pt M_5-edge and Fe K-edge XANES spectra of the as-synthesized nanoparticles in are compared to Pt and Fe standards in Fig. 2. The profile of the Pt M_5-edge in Fig. 2(a) is similar to that of the Pt foil which is an indication of Pt in a metal form. However, the XANES spectra of the Fe K-edge in Fig. 2(b) are entirely different from that of the Fe metal standard but closed to that of hematite (α-Fe_2O_3). The results support the EDS measurements that every sample contains mainly Pt metals and iron oxides with small amount of Fe metals.

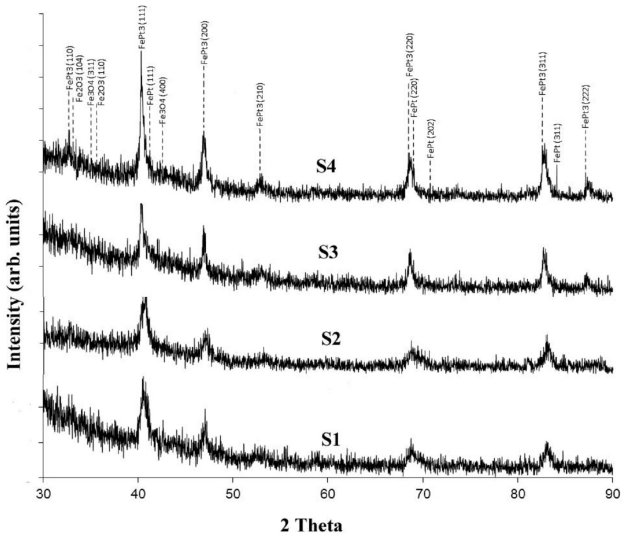

FIGURE 4. X-ray diffraction patterns of nanoparticles synthesized by using (S1) 1.5, (S2) 2.5, (S3) 3.5, and (S4) 4.5 mmol of each surfactant after the annealing at 650°C for 1 hour.

All nanoparticles after the annealing exhibit ferromagnetic properties as shown by hysteresis loops in Fig. 3. However, these ferromagnetic behaviors are primarily related to the particles agglomerations as shown by the TEM images in the insets of S2, S3, S4 in Fig. 3. The sintering of nanoparticles expectedly occurs during the heat treatment at high temperature. In samples S2-S4, the iron oxides are reduced by C that decomposed from a large amount of surfactant molecules [15]. The Fe atoms then diffuse into the particles at high temperature leading to ferromagnetic Fe-rich precipitates much larger than 10 nm. The coercivity, determined from the x-intercept of the hysteresis loops, tends to increase with the increase in surfactants in the synthesis. Interestingly, the agglomeration does not occur in the case of the lowest surfactant concentration (sample S1). In the inset of S1 in Fig. 3, only spheroid iron oxide nanoparticles with size of around 10 nm are increased in number. It follows that the size of FePt and iron oxide nanoparticles above the superparamagnetic limit brings about the enhanced coercivity as high as 1600 Oe. The XRD pattern of this sample also exhibit slight differences around iron oxide peaks from the rest in Fig. 4.

4. Conclusions

Monodisperse magnetic nanoparticles synthesized by the modified polyol process without any reducing agents comprise Pt-rich nuclei and iron oxides. The amount of oleic acid and oleylamine used as surfactants do not significantly affect composition and size of the nanoparticles. However, the nanoparticles have a larger variation in shape when the surfactants are increased. Furthermore, excess surfactants apparently promote the agglomeration of iron oxide and Pt-rich particles during the heat treatment. Nevertheless, the nanoparticles can be transformed to the ferromagnetic phase

without such agglomeration in the case of the lowest surfactants used. These results indicate that the amount of surfactants must be optimized to obtain nanoparticles with desirable morphology and magnetic properties.

Acknowledgements

This work is financially supported by the National Electronics and Computer Technology Center, National Science and Technology Development Agency and Industry/University Cooperative Research Center (I/UCRC) in HDD Component, the Faculty of Engineering, Khon Kaen University with approval of Seagate Technology (Thailand). The authors would like to thank Dr. P. Jantaratana of Kasetsart University for providing VSM facility.

1. B.D. Terris, and T. Thomson, *J. Phys. D: Appl. Phys.* **38** (2005) R199.
2. J. Lopez, F. J. Espinoza-Beltran, G. Zambrano, M.E. Gomez, and P. Prieto, *Rev. Mex. Fis.* **58** (2012) 293.
3. S. Sun, *Adv. Mater.* **18** (2006) 393.
4. A.C.C. Yu, M. Mizuno, Y. Sasaki, and H. Kondo, *Appl. Phys. Lett.* **85** (2004) 6242.
5. K.E. Elkins *et al*., *Nano Lett.* **3** (2003) 1647.
6. C. Liu *et al*., *J. Phys. Chem. B* **108** (2004) 6121.
7. V. Nandwana, K.E. Elkins, and J.P. Liu, *Nanotechnology* **16** (2005) 2823.
8. M. Nakaya, M. Kanehara, and T. Teranishi, *Langmuir* **22** (2006) 3485.
9. L.C. Varanda, and M. Jafelicci, Jr., *J. Am. Chem. Soc.* **128** (2006) 11062.
10. V. Nandwana, K.E. Elkins, N. Poudyal, G.S. Chaubey, K. Yano, and J.P. Liu, *J. Phys. Chem. C* **111** (2007) 4185.
11. K.E. Elkins, G.S. Chaubey, V. Nandwana, and J.P. Liu, *J. Nano Res.* **1** (2008) 23.
12. W. Beck, Jr., C.G.S. Souza, T.L. Silva, M. Jafelicci, Jr., and L.C. Varanda, *J. Phys. Chem. C* **115** (2011) 10475.
13. K. Chokprasombat, C. Sirisathitkul, P. Harding, S. Chandarak, and R. Yimnirun, *J. Nanomater.* **2012** (2012) 758429.
14. S.A. Sebt, S.S. Parhizgar, M. Farahmandjou, P. Aberomand, and M. Akhavan, *J. Supercond. Nov. Magn.* **22** (2009) 849.
15. R. Harpeness, and A. Gedanken, *J. Mater. Chem.* **15** (2005) 698.